Taylor & Francis
Taylor & Francis Group

RESEARCH ARTICLE

🔓 OPEN ACCESS   ✓ Check for updates

Epigallocatechin-3-O-gallate promotes extracellular matrix and inhibits inflammation in IL-1β stimulated chondrocytes by the PTEN/miRNA-29b pathway

Dong Yang, Guanghua Cao, Xiaorong Ba and Haibo Jiang

Department of Orthopaedics, Liyang Peoples' Hospital, Changzhou, PR China

ABSTRACT

Context: Epigallocatechin-3-O-gallate (EGCG) exhibits anti-arthritic activity. MiR-29b-3p provokes chondrocyte apoptosis and promotes the initiation and development of osteoarthritis (OA).

Objective: To explore the roles of EGCG and miR-29b-3p in interleukin-1β (IL-1β)-stimulated chondrocytes.

Materials and methods: HE and Safranin O staining were used to detect the pathological changes of cartilage tissue in OA patients and healthy people. OA-like chondrocyte injury was mimicked by 5 ng/mL IL-1β stimulation for 24 h in vitro, and after transfection with miR-29b-3p mimics and pcDNA-PTEN, IL-1β-stimulated chondrocytes were pre-treated with EGCG (20 and 50 μM) for 2 h. Cell viability, colony numbers, apoptosis rate, the levels of IL-6 and matrix metalloproteinase-13 (MMP-13), miR-19b-3p, PTEN and apoptosis-associated proteins in chondrocytes were evaluated.

Results: MiR-29b-3p level was upregulated in cartilage tissues of OA patients (3.5-fold change, $p < 0.001$) and IL-1β stimulated chondrocytes (two fold change, $p < 0.001$). The matrix staining was weakened and unevenly distributed, and the chondrocytes were arranged disorderly in the tissues of patients with OA. EGCG (20 and 50 μM) increases viability and decreases the levels of miR-29b-3p and MMP-13 and IL-6 in IL-1β stimulated chondrocytes ($p < 0.05$). MiR-29b-3p mimics reversed the effects above 50 μM EGCG ($p < 0.05$). Furthermore, PTEN overexpression abrogated the effects of miR-29b-3p mimics on viability, colony numbers, apoptosis rate and the levels of Bcl-2, MMP-13, IL-6, Bax and cleaved caspase 3 in IL-1β-stimulated chondrocytes ($p < 0.01$).

Discussion and conclusions: EGCG is a potential candidate for the treatment of OA, which also can be explored in a novel therapeutic method for other degenerative or inflammatory disorders.

Introduction

Osteoarthritis (OA), a disease of joint degeneration characterized by articular cartilage (AC) loss, often causes pain, joint stiffness and disability (Liao et al. 2020). In the world, more than 15% of the population suffers from OA (Wu et al. 2019). In addition to various treatment guidelines that have been proposed (McAlindon et al. 2014; Murphy et al. 2016; Ondrésik et al. 2017), no effective strategy exists for the prevention and combat of primary OA, while joint replacement is the most effective therapeutic avenue for end-stage OA (Chen et al. 2017). However, the recovery of impaired AC is a challenge for researchers by virtue of its poor intrinsic healing potential.

Plant-originated agents have attracted increasing attention as a promising therapeutic alternative for their slight side effects and low costs (Zeng et al. 2014). Polyphenols in green tea contain many catechins, the most potent of which is epigallocatechin-3-O-gallate (EGCG) (Yoshimura et al. 2019). EGCG has been reported to possess an array of pharmacological potentials, such as antioxidative (Kaya et al. 2019), anti-inflammatory (Kaya et al. 2019) and anti-arthritic activities (Zheng et al. 2019). In the past decade, Haqqi et al. (1999) as well as Ahmed et al. (2002, 2004), Rasheed et al. (2009), Singh et al. (2010), and

Akhtar and Haqqi (2011), verified that EGCG has cartilage-preserving and chondro-protective activities by extensive researches.

MicroRNAs (miRNAs) are small, noncoding RNAs playing multiple roles in modulation of gene expression at the post-transcriptional level (Pasquinelli 2012). In OA, it has been verified that expression of miRNAs is altered in cartilage pathophysiology and homeostasis (Mirzamohammadi et al. 2014). MiR-29b-3p level is highly up-regulated in cartilage tissue of advanced OA patients (Bobinac et al. 2003). Additionally, miR-29b-3p level in the synovial fluid of OA patients is higher than that in healthy people (Chen and Chen 2019), and such level is elevated in OA tissues and models (Zhi et al. 2021). Chen et al. (2017) proposed that miR-29b-3p provokes apoptosis of chondrocytes and promotes the initiation and progression of OA. Importantly, Rasheed et al. (2018) put forward that the underlying function of EGCG on OA chondrocytes is possibly associated with its capacity to globally repress inflammatory reaction by regulation of miRNAs. EGCG or EGCG-derived compounds could repress cartilage destruction or pain via up-regulating miRNAs in human chondrocytes (Rasheed et al. 2016). Nevertheless, the actions of EGCG on miR-29b-3p expression and the regulatory mechanism involved with EGCG and miR-29b-3p in chondrocytes are still unknown.

CONTACT Dong Yang ✉ yangd_dongyangdyd@163.com 🔵 Department of Orthopaedics, Liyang Peoples' Hospital, No. 70, Jianshe West Road, Liyang, Changzhou, Jiangsu Province 213361, PR China

Our work formulates a goal to reveal the function of EGCG on miR-29b-3p level in interleukin-1β (IL-1β)-stimulated chondrocytes, especially its underlying mechanism in modulating proliferation, apoptosis, inflammation and extracellular matrix (ECM) production. The current study will be conducive to figuring out the specific role and potential mechanism of EGCG in OA-like chondrocytes and offering a promising therapeutic method for OA treatment.

Materials and methods

Ethics statement

Our study was ratified by the Ethics Committee of Liyang People's Hospital (approval number: LY20190416). All experiments conform to the principles outlined in the Declaration of Helsinki (World Medical Association 2013). All subjects voluntarily participated in this study and signed written informed consents.

Clinical information

In this study, five patients with OA who were admitted to our hospital for total knee arthroplasty and five healthy people (traumatic patients without OA and obvious clinical and imaging features) from July 2019 to July 2020 were selected as the research subjects. Among them, OA patients ranged in age from 46 to 68, with an average age of 56.6 years and Kellgren–Lawrence grade III or IV. Healthy people ranged in age from 41 to 67, with an average age of 55.5 years and Kellgren–Lawrence grade 0 or I. The age comparison between OA patients and healthy people was not statistically significant. The joint tissues of each research subject were obtained and stored in −80 °C for subsequent experiments.

Haematoxylin–eosin staining (HE)

The tissue was cut into about 0.5 cm thick and fixed in 4% formaldehyde for 24 h. After that, the tissue sections were placed in xylene for transparency, dehydrated with 70–100% gradient alcohol, and then immersed in paraffin to make embedded blocks. The paraffin embedded tissue was cut into sections about 5 μm thick. Then, the tissue sections were dewaxed by xylene and rehydrated with 100–70% alcohol. The tissue sections were stained with haematoxylin for 10 min, followed by acidification of salt solution for 2 min and then eosin staining for 2 min. The stained sections were dehydrated with alcohol and transparent with xylene, which were then sealed and placed under a microscope (DM2500, Leica, Wetzlar, Germany) to observe the tissue changes.

Safranin O staining

Safranin O staining reagent (TMS-009-C, Sigma-Aldrich, St. Louis, MO) was used to observe the staining of the tissue. The procedure for making tissue sections was the same as that for HE staining. The tissue sections were stained with 0.1% serine for 4 min, washed with water for three times, stained with solid green for 4 min and then washed with glacial acetic acid for 1 min. Then, the tissues were dehydrated with 95% alcohol and 100% alcohol for 10 s. Finally, the tissues were sealed with neutral gum and observed under a microscope.

Cell culture

CHON-001 cells, human OA chondrocyte line (from American Type Culture Collection (ATCC), Manassas, VA), were maintained in complete DMEM medium (11995, Solarbio, Beijing, China) at 37 °C with 5% CO_2.

Treatment of CHON-001 cells

To reveal the role of EGCG in OA-like chondrocyte, CHON-001 cells were divided into control, IL-1β, IL-1β + E20, IL-1β + E50 and E50 groups. Control group: CHON-001 cells were incubated in the absence of IL-1β (SRP6169; Sigma-Aldrich, Shanghai, China) or EGCG (E4143; purity ≥95%; Sigma-Aldrich, Shanghai, China); IL-1β group: CHON-001 cells were incubated in complete DMEM medium and serum-starved for 12 h or overnight and then induced by 5 ng/mL IL-1β for 24 h (Rasheed et al. 2016); IL-1β + E20 group: starved CHON-001 cells were pre-treated with 20 μM EGCG for 2 h prior to stimulation with 5 ng/mL IL-1β for 24 h; IL-1β + E50 group: starved CHON-001 cells were pre-treated with 50 μM EGCG for 2 h prior to stimulation with 5 ng/mL IL-1β for 24 h; E50 group: starved CHON-001 cells were treated with 50 μM EGCG for 2 h. Selection of the EGCG dose was based upon a previous study (Rasheed et al. 2016, 2018).

Next, to determine the effect of EGCG on miR-29b-3p expression in chondrocyte, CHON-001 cells were divided into control, mimics control (MC), miR-29b-3p mimics (M), MC + E50 and M + E50 groups. Control group: CHON-001 cells were incubated without both transfection and EGCG treatment. MC group: CHON-001 cells were only transfected with mimic control. M group: CHON-001 cells were only transfected with M. MC + E50 group: after transfection of mimic control, CHON-001 cells were treated with 50 μM EGCG for 2 h. M + E50 group: after transfection of miR-29b-3p mimic, CHON-001 cells were treated with 50 μM EGCG for 2 h.

To determine the roles of EGCG and miR-29b-3p in OA-like chondrocyte, CHON-001 cells were divided into control, IL-1β, MC, M, MC + IL-1β, MC + IL-1β + E50 and M + IL-1β + E50 groups. Control group: CHON-001 cells were incubated without both transfection and EGCG treatment. IL-1β group: CHON-001 cells were starved overnight and then stimulated with 5 ng/mL IL-1β for 24 h. MC group: CHON-001 cells were only transfected with mimic control. M group: CHON-001 cells were only transfected with miR-29b-3p mimic. MC + IL-1β group: after transfection of MC, starved CHON-001 cells were stimulated with 5 ng/mL IL-1β for 24 h. MC + IL-1β + E50 group: after transfection of mimic control, starved CHON-001 cells were pre-treated with 50 μM EGCG for 2 h prior to stimulation with 5 ng/mL IL-1β for 24 h. M + IL-1β + E50 group: after transfection of miR-29b-3p mimic, starved CHON-001 cells were pre-treated with 50 μM EGCG for 2 h prior to stimulation with 5 ng/mL IL-1β for 24 h.

To examine the effect of EGCG and miR-29b-3p on PTEN expression in OA-like chondrocyte, CHON-001 cells were divided into MC, M, M + IL-1β, MC + IL-1β + E50, MC + IL-1β + E50 and M + IL-1β + E50 groups.

Furthermore, to identify the roles of miR-29b-3p and PTEN in CHON-001 cells, CHON-001 cells were divided into negative control (NC), phosphatase and tensin homolog (PTEN), M, M + IL-1β, M + PTEN and M + IL-1β + PTEN groups. NC group: CHON-001 cells were only transfected with empty vector. PTEN group: CHON-001 cells were only transfected with PTEN

Table 1. Primers used in qRT-PCR.

Gene	RT (5′ → 3′)	Forward (5′ → 3′)	Reverse (5′ → 3′)
miR-29b-3p	GTCGTATCCAGTGCGTGTCGTGGAGTCGGCAATTGCACTGGATACGACTAACCGAT	AGCACCATCTGAAATCGGTT	TGTCGTGGAGTCGGCAATTG
U6	CGCTTCACGAATTTGCGTGTCAT	CGCTTCACGATTTGCGTGTCAT	GCTTCGGCAGCACATATACTAAAAT
hsa-PTEN	Random hexamer	CCGAAAGGTTTTGCTACCATTCT	AAAATTATTTCCTTTCTGAGCATTCC
hsa-GAPDH	Random hexamer	CACCACACTGAATCTCCCCT	TGGTTGAGCACAGGGTACTT

plasmid. M group: CHON-001 cells were only transfected with miR-29b-3p mimic. M + IL-1β group: after transfection of mimic control, starved CHON-001 cells were stimulated with 5 ng/mL IL-1β for 24 h. M + PTEN group: CHON-001 cells were co-transfected with miR-29b-3p mimic and PTEN plasmid. M + IL-1β + PTEN group: after transfection of miR-29b-3p mimic and PTEN plasmid, starved CHON-001 cells were stimulated with 5 ng/mL IL-1β for 24 h.

Transfection

CHON-001 cells were transfected with 50 nM miR-29b-3p mimics (miR10000100-1-5) or 50 nM miRNA MC (miR1N0000001-1-5) which were purchased from RiboBio (Guangzhou, China). The target gene fragments of PTEN were amplified and cloned into pcDNA3.1 vector (V79020, ThermoFisher, Waltham, MA) by RiboBio (Guangzhou, China) to construct overexpression plasmid containing the PTEN sequence (pcDNA-PTEN). Empty pcDNA3.1 vector was denoted as NC for pcDNA-PTEN. CHON-001 cells were transfected with constructs for 24 h using riboFECT CP Transfection Kit (C10511-05, RiboBio, Guangzhou, China).

Bioinformatics prediction and dual-luciferase reporter assay

The binding correlation between miR-29b-3p and PTEN was predicted by TargetScan V7.2 (http://www.targetscan.org/vert_72/). Both wild type (WT) and the mutants (MUT) of the 3′-UTRs of PTEN were cloned into pmirGLO vector (E1330, Promega, Madison, WI). The full length of PTEN 3′UTR-WT was 5′-TTTTTTAAAGCATATTGGTGCTA-3′, while that of PTEN 3′UTR-MUT was 5′-TTTTTTAAAGCATATCAAGTAGA-3′. All constructs were transfected into 293T cells (ATCC) with miR-29b-3p mimics using riboFECT CP Transfection Kit for 6 h. The luciferase activity was determined by a microplate reader (Bio-rad 550, Bio-Rad, Hercules, CA).

Cell viability

Viability of CHON-001 cells was evaluated by cell counting kit-8 (CCK-8) (CK04, Dojindo Molecular Technologies, Tokyo, Japan). Treated or untreated CHON-001 cells were grown for 48 h in a 96-well plate. After that, each well was added with CCK-8 solution (10 μL). Four hours later, absorbance was detected using a microplate reader (Bio-rad 550, Bio-Rad, Hercules, CA) at 450 nm.

ELISA

Human matrix metalloproteinase-13 (MMP-13) (EK0468) and interleukin-6 (IL-6) (EK0410) specific ELISA kits were obtained from Wuhan Boshide Bioengineering Co., Ltd. (Wuhan, China). MMP-13 and IL-6 produced in the culture medium were quantified with commercially corresponding ELISA kits. Absorbance

was measured using a microplate reader (Bio-rad 550, Bio-Rad, Hercules, CA) at 450 nm.

Colony formation assay

After treatment, 1×10^3 CHON-001 cells were re-plated in a 35-mm dish in duplicate and incubated at 37 °C with 5% CO_2. When colonies became visible to the naked eye, the plates were fixed by adding 200 μL 4% paraformaldehyde (P0099, Beyotime, Shanghai, China) for 15 min and stained with 200 μL 0.5% crystal violet (C8470, Solarbio, Beijing, China) for 15 min at 37 °C. The colony numbers were counted under microscope (IX71 inverted microscope; Olympus, Shinjuku, China).

Flow cytometry analysis

The apoptosis of cells was determined with Annexin V-FITC Apoptosis Detection Kit (CA1020, Solarbio, Beijing, China). One millilitre of cells suspension (a density of 1×10^6 cells/mL) was centrifuged at $1000 \times g$ for 5 min at 4 °C. Following discarding the supernatant, a total of 1 mL precooled PBS buffer was added. Then, the mixture was centrifuged again and supernatant was discarded. These procedures were repeated twice. Subsequently, cells were resuspended with 200 μL binding buffer, and then stained with 10 μL Annexin V-FITC and 10 μL propidium iodide (PI) in the dark for 15 min at 37 °C. After that, 300 μL binding buffer solution was added and the apoptosis of cells was determined by flow cytometer CytoFLEX (Beckman Coulter Life Science, Milan, Italy).

Real-time reverse transcription polymerase chain reaction (qRT-PCR)

Total RNA was isolated from tissues and CHON-001 cells with the Trizol reagent (15596-026, Invitrogen, Carlsbad, CA). Reverse transcription (RT) reactions for mRNAs were performed using GoScript RT System (A5000, Promega, Madison, WI), with random primers and oligo dT. RT reaction for miR-29b-3p was carried out by PrimeScript RT reagent Kit (RR047A, TaKaRa, Dalian, China), with a stem-loop primer (Table 1). Then, the levels of gene expression was quantified by standard real-time PCR protocol with GoTaq qPCR Master Mix (A6002, Promega, Madison, WI) in Applied Biosystems 7500 Real-time PCR System (Applied Biosystems, Waltham, MA) as per the manufacturer's protocol. GAPDH or U6 was used as a reference gene for mRNA or miRNA, respectively. Gene expression levels were calculated using the $2^{-\Delta\Delta Ct}$ method (Livak and Schmittgen 2001). Table 1 includes primer sequences.

Western blot

The proteins were lysed from cells by RIPA buffer (P0013E, Beyotime, Shanghai, China), isolated by 12% SDS-PAGE, and then electrotransferred onto PVDF membranes (YA1701, Solarbio, Beijing, China). Membranes were incubated in 5% (v/v)

Table 2. List of primary antibodies used for Western blots.

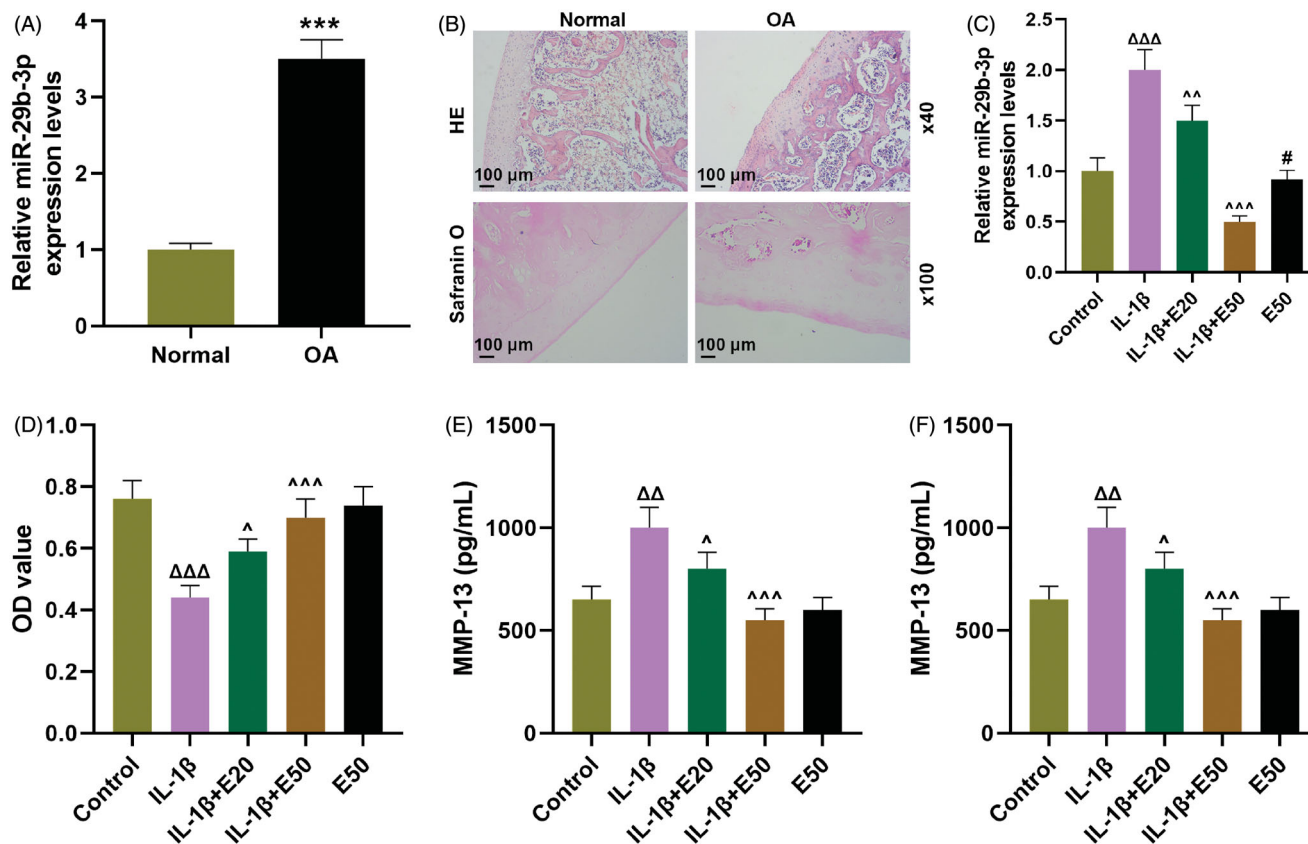| Protein	Antibody	Catalogue number	Company	Antibody dilution
Bcl-2	Rabbit anti-Bcl-2 antibody	ab59348	Abcam	1:1000
Bax	Rabbit anti-Bax antibody	ab32503	Abcam	1:1000
Cleaved (C)-caspase-3	Rabbit anti-cleaved caspase-3 antibody	ab2302	Abcam	1:500
PTEN	Rabbit anti-PTEN antibody	ab32199	Abcam	1:10,000
GAPDH	Rabbit anti-GAPDH antibody	ab181602	Abcam	1:10,000

Figure 1. EGCG inhibited the levels of miR-29b-3p, MMP-13 and IL-6β but promoted cell viability on IL-1β-stimulated CHON-001 cells. (A) MiR-29b-3p expression in OA tissues and normal tissue was detected by qRT-PCR. (B) HE and Safranin O staining were used to detect the pathological changes of cartilage tissue in OA patients and healthy people. (C) The level of miR-29b-3p was determined by qRT-PCR in CHON-001 cells. (D) Cell counting kit-8 (CCK-8) indicated cell viability in CHON-001 cells. (E, F) The levels of MMP-13 and IL-6 were determined by ELISA in CHON-001 cells. U6 was used as a reference gene for miRNA. EGCG: epigallocatechin-3-O-gallate; EGCG20: 20 μM EGCG; EGCG50: 50 μM EGCG; qRT-PCR: real-time reverse transcription polymerase chain reaction; ELISA: enzyme-linked immunosorbent assay; control: CHON-001 cells cultured without IL-1β or EGCG. $^{\triangle\triangle\triangle}p < 0.001$ vs. control; $^{\wedge}p < 0.05$ or $^{\wedge\wedge}p < 0.01$ or $^{\wedge\wedge\wedge}p < 0.001$ vs. IL-1β. All measurements were performed at least three times. Data were presented as the means ± standard deviation (SD).

skimmed milk and then probed with primary antibodies (Table 2) overnight at 4 °C. After probing with Goat Anti-Rabbit IgG H&L (HRP) (ab205718, 1:2000, Abcam, Waltham, MA), protein blots were visualized by ECL Western Blotting Substrate (32209, Thermo Fisher Scientific, Waltham, MA) and digitized by NIH Image (National Institutes of Health, Bethesda, MD). GAPDH was used as a loading control.

Statistical analysis

All measurements were performed at least three times. Data were expressed as the means ± standard deviation (SD). Statistical analyses were performed by Prism 8.0.2 (GraphPad Inc., La Jolla, CA) and $p < 0.05$ was considered as statistically significant. Student's t-test was employed for measuring the difference between two groups, whereas one-way ANOVA analysis followed by Tukey's post hoc analysis was conducted to analyse comparisons between three or more groups.

Results

EGCG inhibited the levels of miR-29b-3p, MMP-13 and IL-6 but promoted cell viability in IL-1β-stimulated CHON-001 cells

First of all, the miR-29b-3p expression in OA tissues and normal tissue was detected by qRT-PCR, the results of which indicated that miR-29b-3p expression was markedly up-regulated in OA tissues compared to normal tissue (Figure 1(A), $p < 0.001$). HE and Safranin O staining were used to detect the pathological changes of cartilage tissue in OA patients and healthy people. The results demonstrated that the AC structure of the normal group was intact and the matrix components were evenly distributed. In the tissues of patients with OA, the matrix staining was weakened and unevenly distributed, with disordered arrangement of chondrocytes (Figure 1(B), $p < 0.001$). After stimulating with IL-1β, the level of miR-29b-3p was strikingly increased in CHON-001 cells (Figure 1(C), $p < 0.001$). By contrast, this effect

was partially offset by EGCG (Figure 1(C), $p < 0.001$). IL-1β notably decreased viability of CHON-001 cells (Figure 1(D), $p < 0.001$), whereas such inhibition of IL-1β was obviously alleviated by EGCG (Figure 1(D), $p < 0.05$). MMP-13 and IL-6 expression was up-regulated in CHON-001 cells following IL-1β treatment (Figure 1(E,F), $p < 0.001$), which was partially eliminated by EGCG (Figure 1(E,F), $p < 0.01$).

EGCG inhibited the levels of miR-29b-3p, MMP-13 and IL-6β but promoted viability in IL-1β-stimulated CHON-001 cells by the down-regulation of miR-29b-3p

MiR-29b-3p mimics as well as IL-1β and miR-29b-3p mimics strikingly promoted the level of miR-29b-3p in CHON-001 cells (Figure 2(A), $p < 0.001$; Figure 2(B), $p < 0.001$), which was partially reversed by EGCG (Figure 2(A), $p < 0.001$). Specifically, EGCG significantly attenuated IL-1β or miR-29b-3p mimics-induced increase in miR-29b-3p level related to MC + IL-1β group (Figure 2(B), $p < 0.001$) or M + IL-1β group (Figure 2(B), $p < 0.001$), respectively. Moreover, both IL-1β and miR-29b-3p

mimics (Figure 2(C), $p < 0.001$) remarkably decreased viability in CHON-001 cells, which were obviously attenuated by EGCG as compared to MC + IL-1β group (Figure 2(C), $p < 0.001$) or M + IL-1β group (Figure 2(C), $p < 0.001$). Moreover, both IL-1β (Figure 2(D,E), $p < 0.001$) and miR-29b-3p mimics (Figure 2(D,E), $p < 0.01$) dramatically promoted the levels of MMP-13 and IL-6 in CHON-001 cells. In contrast, EGCG significantly attenuated IL-1β or miR-29b-3p mimics-induced increase in the levels of MMP-13 and IL-6 compared to MC + IL-1β group or M + IL-1β group (Figure 2(D,E), $p < 0.001$), respectively.

EGCG indirectly increased PTEN expression via decreasing miR-29b-3p in IL-1β-stimulated CHON-001 cells

The binding correlation between miR-29b-3p and PTEN was predicted by TargetScan (Figure 3(A)) and verified by dual-luciferase reporter assay (Figure 3(B), $p < 0.001$). IL-1β obviously inhibited the mRNA and protein expression levels of PTEN in CHON-001 cells (Figure 3(C–E), $p < 0.001$), which was partially abrogated by EGCG in a concentration-dependent manner
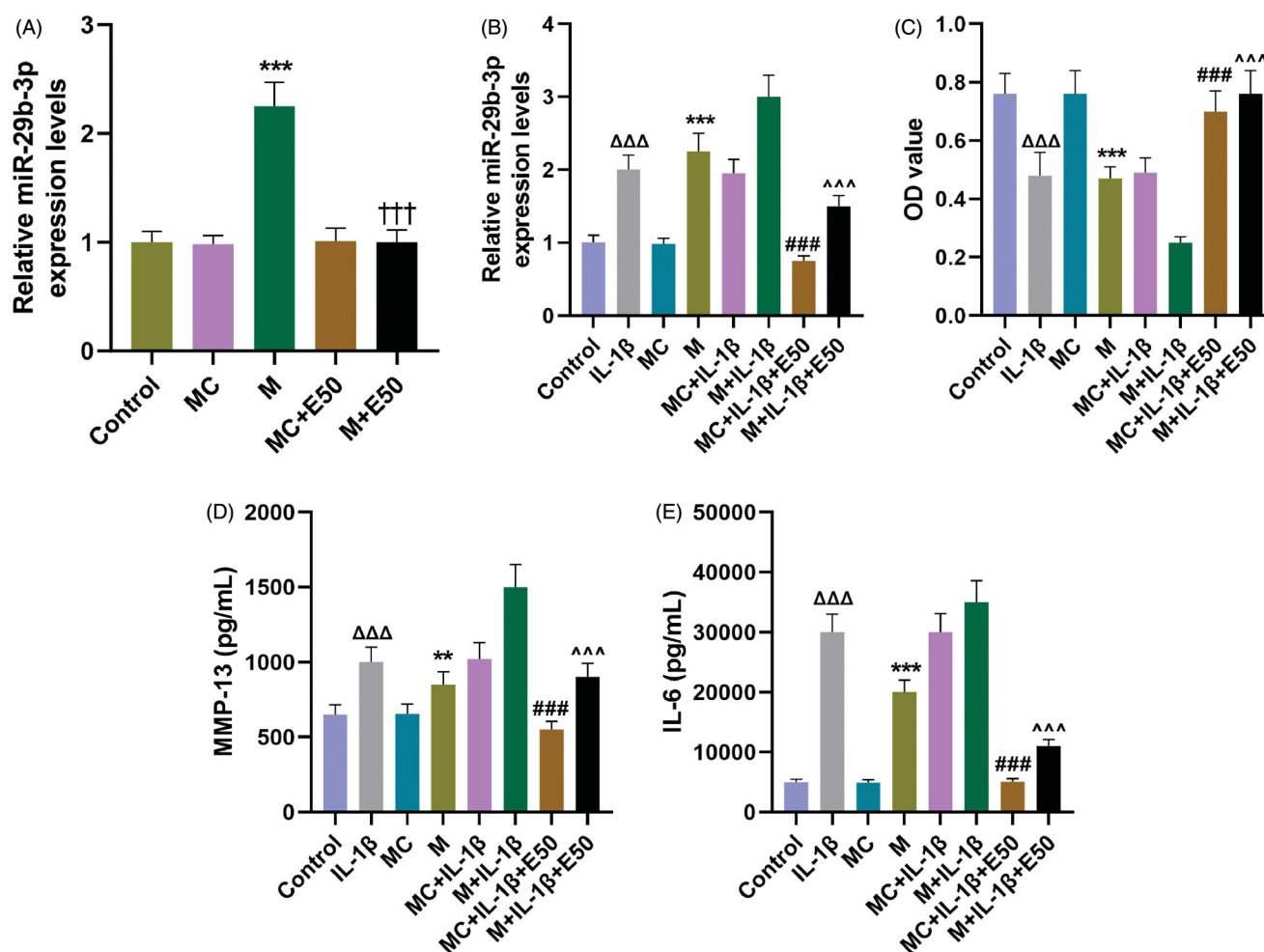

Figure 2. EGCG inhibited the levels of miR-29b-3p, MMP-13 and IL-6β but promoted cell viability in IL-1β-stimulated CHON-001 cells by the down-regulation of miR-29b-3p. (A) CHON-001 cells were divided into control, MC, M, MC + E50 and M + E50 groups. (B–E) CHON-001 cells were divided into control, IL-1β, MC, M, MC + IL-1β, M + IL-1β, MC + IL-1β + E50 and M + IL-1β + E50 groups. (A, B) The level of miR-29b-3p was determined by qRT-PCR in CHON-001 cells. (C) Cell counting kit-8 (CCK-8) indicated cell viability in CHON-001 cells. (D, E) The levels of MMP-13 and IL-6 were determined by ELISA in CHON-001 cells. U6 was used as a reference gene for miRNA. EGCG: epigallocatechin-3-O-gallate; E50: 50 μM EGCG; MC: mimics control; M: miR-29b-3p mimics; qRT-PCR: real-time reverse transcription polymerase chain reaction; control: CHON-001 cells cultured without IL-1β or EGCG. $^{\triangle\triangle\triangle}p < 0.001$ vs. control; $^{**}p < 0.01$ or $^{***}p < 0.001$ vs. MC; $^{\dagger\dagger\dagger}p < 0.001$ vs. M; $^{\wedge\wedge}p < 0.001$ vs. M + IL-1β. All measurements were performed at least three times. Data were presented as the means ± standard deviation (SD).
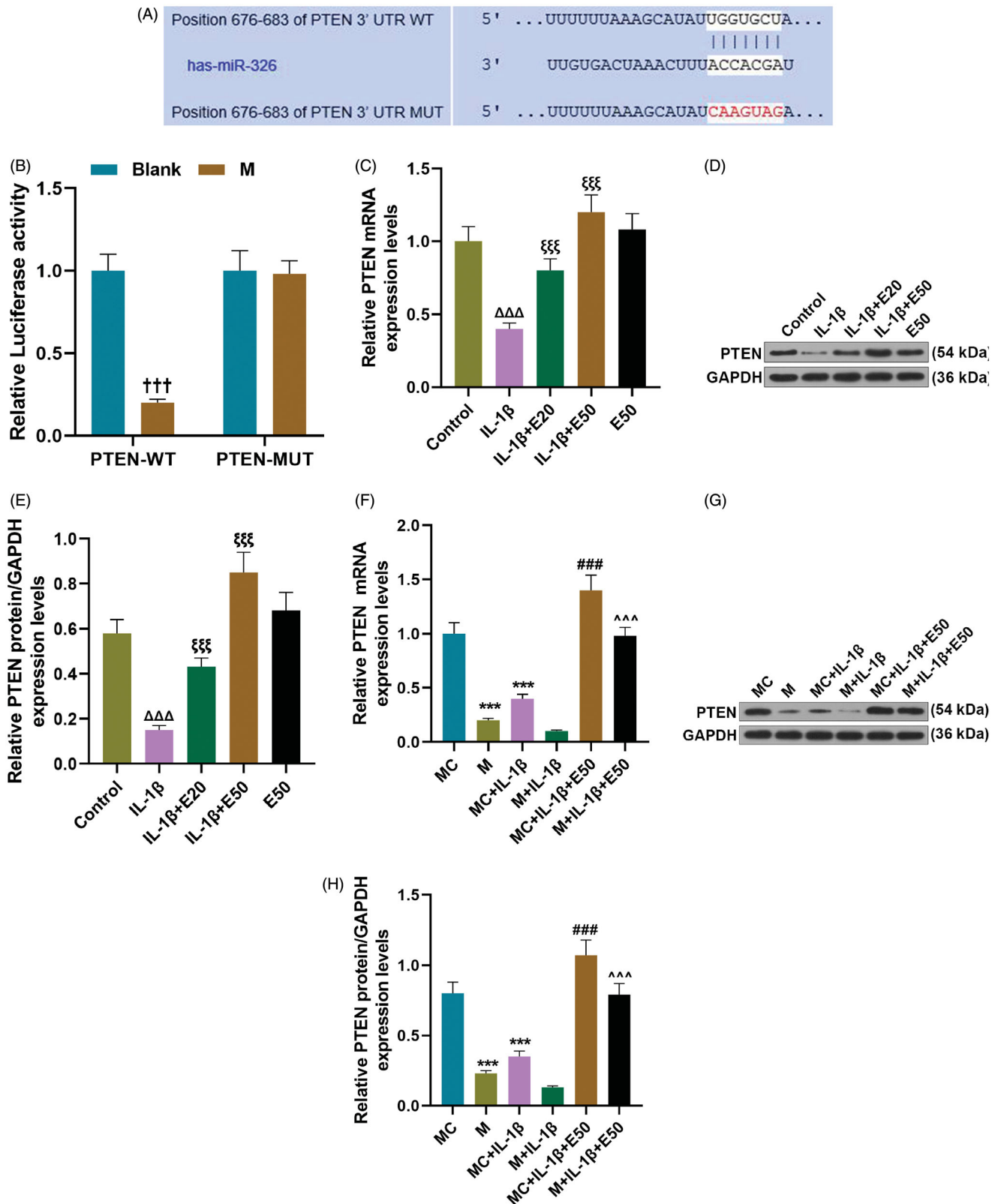
Figure 3. EGCG indirectly increased phosphatase and tensin homolog (PTEN) expression via decreasing miR-29b-3p in IL-1β-stimulated CHON-001 cells. (A, B) The binding relationship between miR-29b-3p and PTEN was predicted by TargetScan V7.2 (A) and verified by dual-luciferase reporter assay (B). (C–E) CHON-001 cells were divided into control, IL-1β, IL-1β + E20, IL-1β + E50 and E50 groups. The protein (C, D) and mRNA (E) levels of PTEN in CHON-001 cells were determined by qRT-PCR and Western blot, respectively. (F–H) CHON-001 cells were divided into MC, M, MC + IL-1β, M + IL-1β, MC + IL-1β + E50 and M + IL-1β + E50 groups. The protein (F, G) and mRNA (H) levels of PTEN in CHON-001 cells were determined by qRT-PCR and Western blot, respectively. GAPDH was used as the internal reference control for PTEN. EGCG: epigallocatechin-3-O-gallate; E50: 50 μM EGCG; MC: mimics control; M: miR-29b-3p mimics; qRT-PCR: real-time reverse transcription polymerase chain reaction; control: CHON-001 cells cultured without IL-1β or EGCG. $^{†††}p < 0.001$ vs. blank; $^{ΔΔΔ}p < 0.001$ vs. control; $^{ξξξ}p < 0.001$ vs. IL-1β; $^{**}p < 0.01$ or $^{***}p < 0.001$ vs. MC; $^{∧∧∧}p < 0.001$ vs. M + IL-1β. All measurements were performed at least three times. Data were presented as the means ± standard deviation (SD).
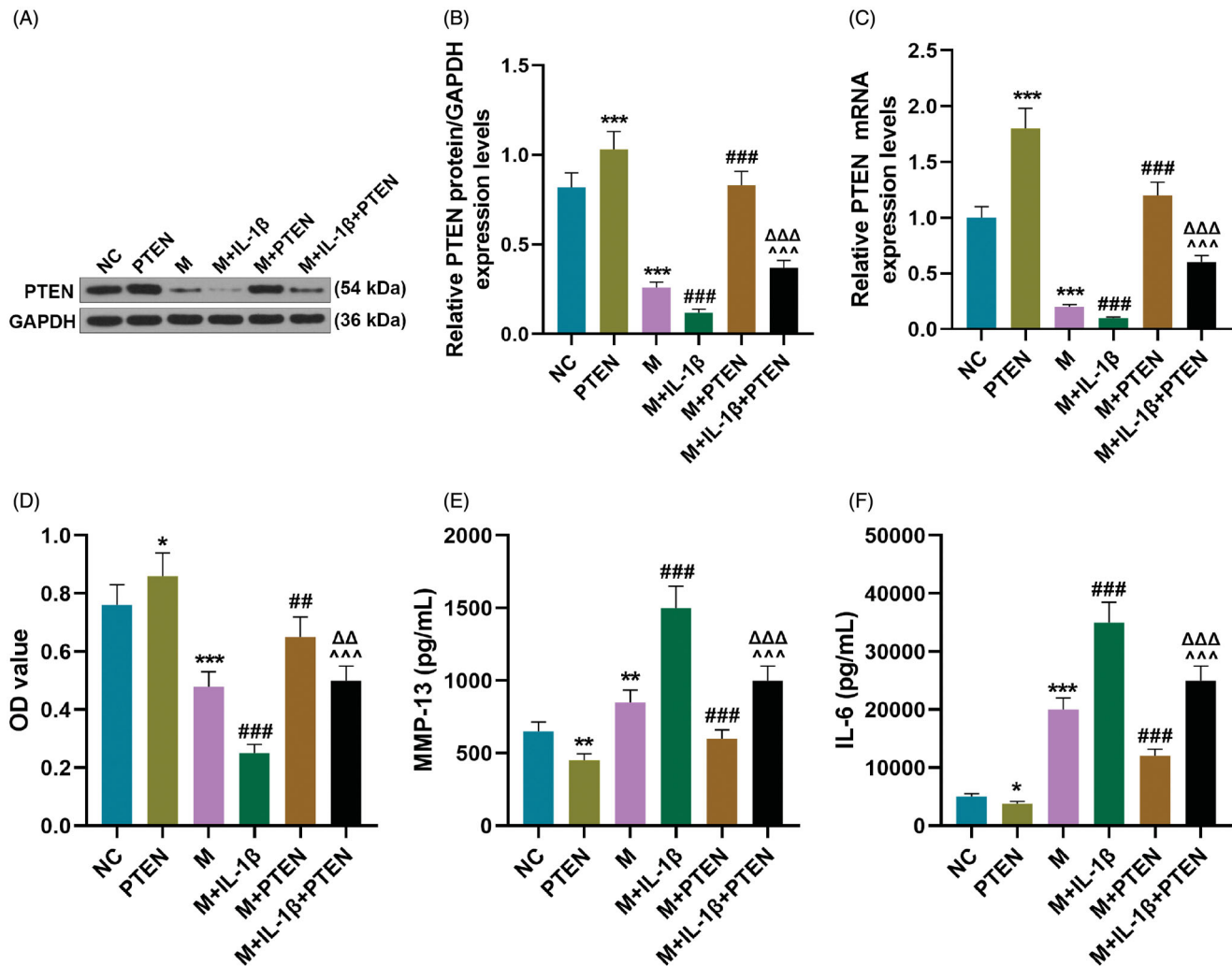
Figure 4. Overexpressed miR-29b-3p affected viability and the levels of MMP-13 and IL-6 of IL-1β-stimulated CHON-001 cells via down-regulating PTEN. (A–F) CHON-001 cells were divided into NC, PTEN, M, M + IL-1β, M + PTEN and M + IL-1β + PTEN groups. The protein (A, B) and mRNA (C) levels of PTEN in CHON-001 cells were determined by Western blot and qRT-PCR, respectively. (D) Cell counting kit-8 (CCK-8) assay indicated viability of CHON-001 cells. (E, F) The levels of MMP-13 and IL-6 were determined by ELISA in CHON-001 cells. GAPDH was used as the internal reference control for PTEN. MC: mimics control; M: miR-29b-3p mimics; qRT-PCR: real-time reverse transcription polymerase chain reaction; ELISA: enzyme-linked immunosorbent assay. $*p < 0.05$ or $**p < 0.01$ or $***p < 0.001$ vs. NC; $^{\wedge\wedge\wedge}p < 0.001$ vs. M + IL-1β; $^{\Delta\Delta\Delta}p < 0.001$ vs. M + PTEN. All measurements were performed at least three times. Data were presented as the means ± standard deviation (SD).

(Figure 3(C–E), $p < 0.001$). In CHON-001 cells, PTEN expression was strikingly downregulated by overexpressed miR-29b-3p (Figure 3(F–H), $p < 0.001$), but was significantly up-regulated in M + IL-1β + E50 group as compared to that in M + IL-1β group (Figure 3(F–H), $p < 0.001$). It can be concluded from the results that EGCG indirectly elevated PTEN expression via decreasing miR-29b-3p in IL-1β-stimulated CHON-001 cells.

The effect of overexpressed miR-29b-3p on viability, and the levels of MMP-13 and IL-6 in IL-1β-stimulated CHON-001 cells via down-regulating PTEN

In IL-1β-stimulated CHON-001 cells, overexpressed miR-29b-3p strikingly inhibited PTEN expression (Figure 4(A–C), $p < 0.001$) and viability (Figure 4(D), $p < 0.001$) but promoted the levels of MMP-13 and IL-6 (Figure 4(E,F), $p < 0.01$), which was partially abrogated by overexpressed PTEN (Figure 4(A–C), $p < 0.001$; Figure 4(D), $p < 0.001$; Figure 4(E,F), $p < 0.001$).

Overexpressed miR-29b-3p repressed proliferation and promoted apoptosis in IL-1β-stimulated CHON-001 cells via down-regulating PTEN

In IL-1β-stimulated CHON-001 cells, the proliferation was significantly inhibited (Figure 5(A), $p < 0.05$) while the apoptosis was obviously promoted (Figure 5(B), $p < 0.001$) by up-regulation of miR-29b-3p, which were partially offset by overexpressed PTEN (Figure 5(A), $p < 0.01$; Figure 5(B), $p < 0.001$).

Overexpressed MiR-29b-3p regulated the expression of apoptosis-related proteins in IL-1β-stimulated CHON-001 cells by down-regulating PTEN

Overexpressed miR-29b-3p obviously promoted the protein expressions of Bax and cleaved (C) caspase 3 (Figure 6(A,B), $p < 0.01$), but inhibited the protein expression of Bcl-2 in IL-1β-stimulated CHON-001 cells (Figure 6(A,B), $p < 0.001$). On the contrary, these effects were partially offset by overexpressed PTEN (Figure 6(A,B), $p < 0.001$).
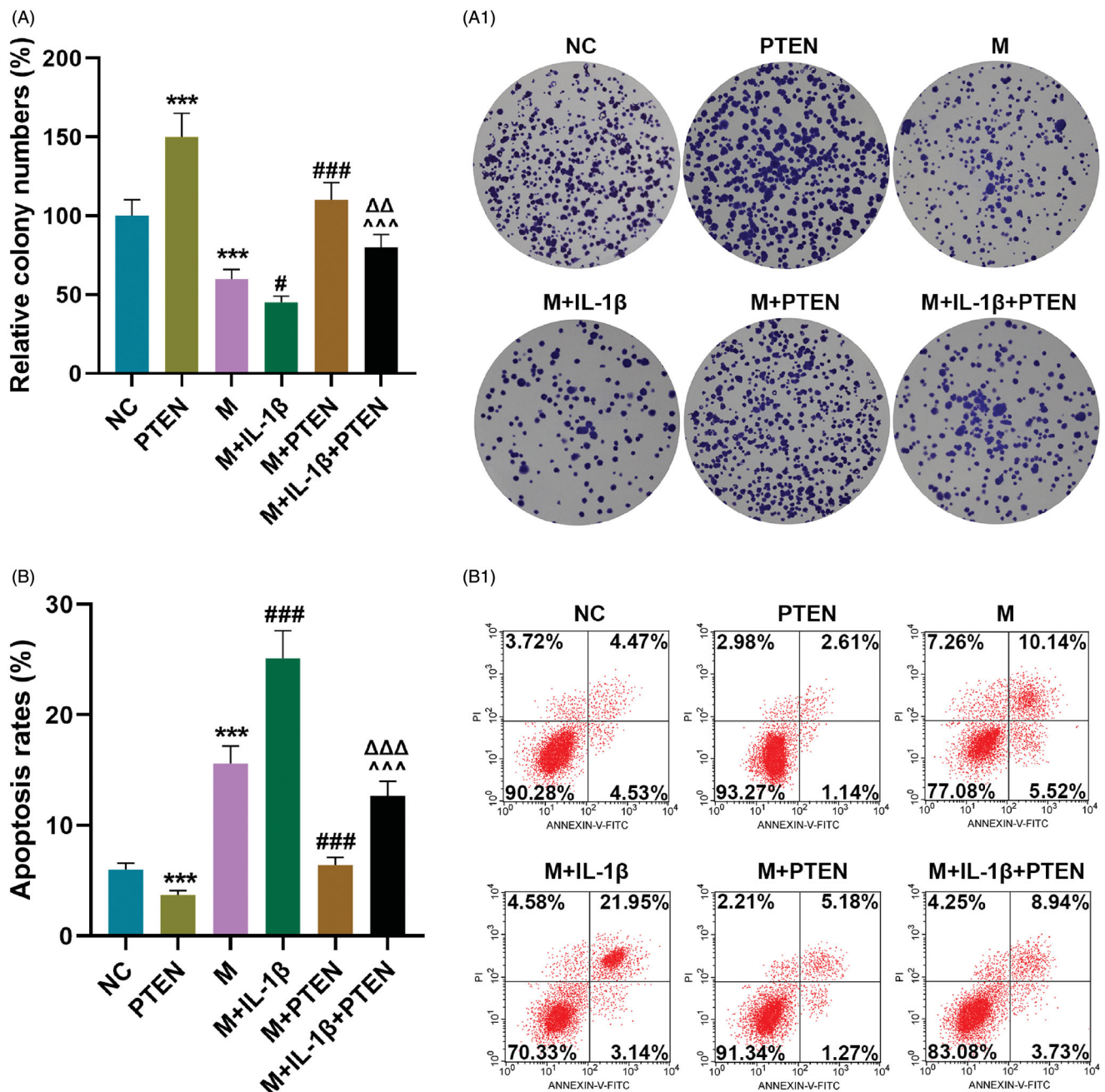
Figure 5. Overexpressed miR-29b-3p inhibited proliferation and promoted apoptosis in IL-1β-stimulated CHON-001 cells via down-regulating PTEN. (A, B) CHON-001 cells were divided into NC, PTEN, M, M + IL-1β, M + PTEN and M + IL-1β + PTEN groups. Colony numbers (A) and apoptosis rate (B) of CHON-001 cells were determined by colony formation and flow cytometry assays, respectively. MC: mimics control; M: miR-29b-3p mimics; NC: negative control. ***$p < 0.001$ vs. NC; #$p < 0.05$ or ###$p < 0.001$ vs. M; ^^^$p < 0.001$ vs. M + IL-1β; ΔΔ$p < 0.01$ or ΔΔΔ$p < 0.001$ vs. M + PTEN. All measurements were performed at least three times. Data are presented as the means ± standard deviation (SD).

Discussion

AC is primarily composed of chondrocytes and ECM. Chondrocytes promote ECM synthesis or degradation through generating anabolic or catabolic factors (Goldring et al. 2011). Chondrocytes play a critical role in AC deterioration and the pathological progression of OA (Findlay and Atkins 2014). OA severity is associated with increased expression of certain pro-inflammatory factors, like IL-6 (Geurts et al. 2018). Inflammatory factors exhibit a damaging effect on cartilage by suppressing anabolic activities of chondrocytes (Saklatvala 1986; Guerne et al. 1990), and activate chondrocytes to synthetize matrix metalloproteinase (MMPs), particularly MMP-13, a critical regulator of cartilage deterioration (Mengshol et al. 2000). Fibrillar collagens I, II (Col II) and III are the main components of the ECM (Manka et al. 2019). ECM was actively remodelled and degraded by secreting extracellular MMPs. Cleavage of Col II is believed as a key event in the early stages of OA, with the initial Col II cleavage being preferentially carried out by MMP-13 (Xiao et al. 2019).

By performing *in vivo* research, diets containing naturally sourced agents in animals were observed to modulate the expressions of miRNAs (Sethi et al. 2013). In breast cancer cells, EGCG down-regulated the level of miR-25 (Zan et al. 2019). EGCG might function as an anti-hepatitis C virus agent that reduces cellular infectivity by up-regulating miR-548m (Mekky
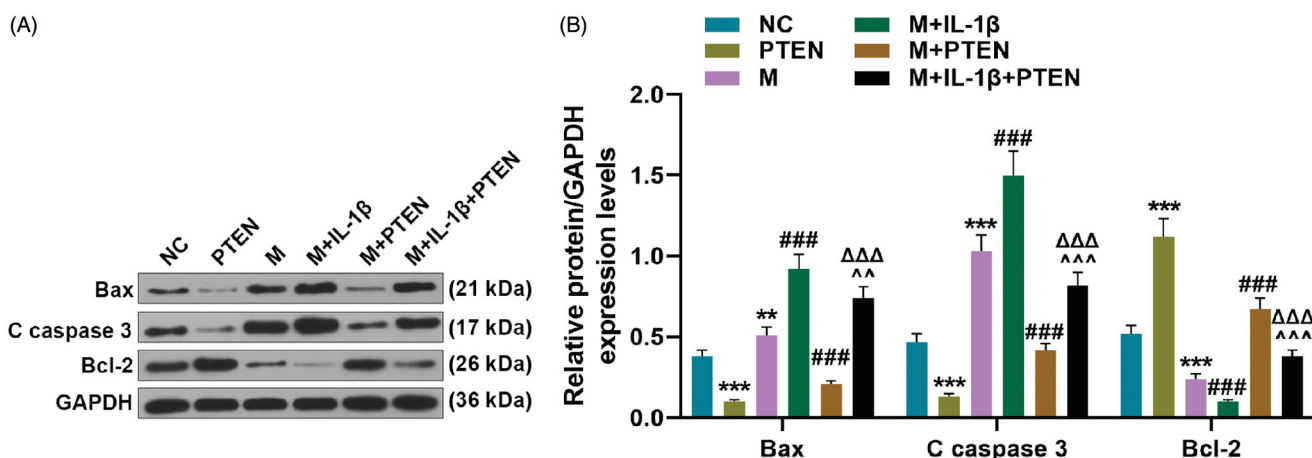
(A)

(B)

Figure 6. Overexpressed miR-29b-3p regulated the expression of apoptosis-related proteins in IL-1β-stimulated CHON-001 cells via down-regulating PTEN. (A, B) CHON-001 cells was divided into NC, PTEN, M, M + IL-1β, M + PTEN and M + IL-1β + PTEN groups. The expression of apoptosis-related proteins (Bax, cleaved (C) caspase 3 and Bcl-2) were determined by Western blot. GAPDH was used as the internal reference control for PTEN. MC: mimics control; M: miR-29b-3p mimics; NC: negative control. $**p < 0.01$ or $***p < 0.001$ vs. NC; $###p < 0.001$ vs. M; $^{\wedge\wedge}p < 0.01$ or $^{\wedge\wedge\wedge}p < 0.001$ vs. M + IL-1β; $^{\Delta\Delta\Delta}p < 0.001$ vs. M + PTEN. All measurements were performed at least three times. Data are presented as the means ± standard deviation (SD).

et al. 2019). In the present study, OA-like chondrocyte injury was mimicked by IL-1β stimulation *in vitro* and IL-1β-stimulated chondrocytes were treated with EGCG or/and transfected with miR-29b-3p mimics. The current study proved that miR-29b-3p was highly expressed in IL-1β-stimulated chondrocytes, which is consistent with a recent report that miR-29b-3p is overexpressed in cartilage tissue from OA patients (Chen et al. 2017). Additionally, EGCG strikingly attenuated IL-1β or/and miR-29b-3p up-regulation-induced decrease in cell viability, and IL-1β or/and miR-29b-3p overexpression-mediated increase in the levels of miR-29b-3p, MMP-13 and IL-6. The findings suggested that EGCG can inhibit ECM degradation and inflammatory response in IL-1β-stimulated chondrocytes via increasing cell viability, and decreasing MMP-13 and IL-6 levels by down-regulating miR-29b-3p.

Further mechanism exploration in our work revealed that PTEN was a direct target of miR-29b-3p. Consistent with previous work (Hou et al. 2020; Xia et al. 2020), our findings confirmed that overexpressed miR-29b-3p could inhibit PTEN expression. Moreover, EGCG increased PTEN expression through inhibiting miR-29b-3p expression in IL-1β-induced chondrocytes. Here, we demonstrated that overexpressed miR-29b-3p further promoted IL-1β-induced decrease in viability and increase in miR-29b-3p, MMP-13 and IL-6 levels, which, however, were partially offset by overexpressed PTEN. The data suggested that up-regulated miR-29b-3p significantly reduced cell viability and augmented the levels of miR-29b-3p, MMP-13 and IL-6 through down-regulating PTEN in IL-1β-stimulated chondrocytes.

Promoting proliferation and inhibiting apoptosis in chondrocytes have been the critical methods to halt and control the progression of OA (Jin et al. 2014; Yan et al. 2016). Inflammatory cytokines tend to provoke apoptosis of chondrocytes (Héraud et al. 2000; López-Armada et al. 2006). Some researchers reported that apoptosis of chondrocyte occurred in late stages of OA (Zamli et al. 2013), while others reported that it occurred in early stages of OA (Loening et al. 2000). In spite of that, the positive relationship between apoptosis of chondrocyte and the severity of OA has been reported. Thus, elevated chondrocyte apoptosis is a primary characteristic of OA, and preventing chondrocyte apoptosis is regarded to be a potent way to attenuate OA (Shi et al. 2017; Cao et al. 2018). We observed that up-

regulated miR-29b-3p notably repressed proliferation and provoked apoptosis through down-regulating PTEN in IL-1β-stimulated chondrocytes. Furthermore, overexpressed miR-29b-3p strikingly promoted Bax expression but inhibited C caspase 3 and Bcl-2 expressions through down-regulating PTEN in IL-1β-stimulated chondrocytes. Apoptosis is modulated by activation of apoptotic cascade by caspase-3 whose cleaved protein is believed as an executioner of apoptotic signal and an essential for promotion of apoptosis (Dolka et al. 2016). Bcl-2 and Bax, the members of the Bcl-2 family of proteins, can regulate apoptosis and attenuate caspase-3 activation (Liu et al. 2017). Thus, overexpressed miR-29b-3p inducted apoptosis in chondrocytes through regulating apoptosis-related proteins.

This study demonstrates that EGCG inhibited inflammatory response, degradation of ECM and decrease of cell numbers in OA-like chondrocytes by up-regulating PTEN via down-regulating miR-29b-3p. These findings support the potential of EGCG as an anti-arthritic agent for prevention or control of OA or other degenerative disorders. MiR-29b-3p and PTEN may serve as potential targets for OA treatment. It has been reported that the inhibitory effects of EGCG on inflammatory response in human chondrocytes could be mediated by inhibiting the activation of NF-κB and c-Jun N-terminal Kinase (JNK)-MAPK (Akhtar and Haqqi 2011). Other results identify new promising targets of EGCG in the treatment of OA chondrocytes, including miR-140-3p and ADAMTS5 (Rasheed et al. 2018), miR-199a-3p and cyclooxygenase (COX)-2 (Rasheed et al. 2016). Thus, it is also possible that other regulatory pathways are involved in the regulation of PTEN/miRNA-29b pathway by EGCG. These possibilities require future study. Besides, there are several limitations to the study. The main limitation of this study was the small sample size of clinical cases. Another limitation in this study is the lack of animal experiments and human studies. Further exploration about the role and toxicity of EGCG with an appropriate animal model should be performed in the future.

Conclusions

The present study suggested that EGCG may contribute to the repair and regeneration of damaged AC through increasing numbers of chondrocytes and decreasing ECM degradation and inflammatory response. The effects of EGCG on OA depended

on the mechanism that EGCG may promote proliferation and inhibit apoptosis, followed by the decreases of MMP-13, IL-6, Bax and C caspase 3 levels and the increase of Bcl-2 level, through up-regulating PTEN via down-regulating miR-29b-3p in IL-1β-stimulated chrondrocytes. This can be explored as a newer therapeutic method for the prevention or control of OA and other degenerative or inflammatory disorders.

Disclosure statement

The authors declare no conflicts of interest.

Funding

References

Ahmed S, Rahman A, Hasnain A, Lalonde M, Goldberg VM, Haqqi TM. 2002. Green tea polyphenol epigallocatechin-3-gallate inhibits the IL-1 beta-induced activity and expression of cyclooxygenase-2 and nitric oxide synthase-2 in human chondrocytes. Free Radic Biol Med. 33(8): 1097–1105.

Ahmed S, Wang N, Lalonde M, Goldberg VM, Haqqi TM. 2004. Green tea polyphenol epigallocatechin-3-gallate (EGCG) differentially inhibits interleukin-1 beta-induced expression of matrix metalloproteinase-1 and -13 in human chondrocytes. J Pharmacol Exp Ther. 308(2):767–773.

Akhtar N, Haqqi TM. 2011. Epigallocatechin-3-gallate suppresses the global interleukin-1beta-induced inflammatory response in human chondrocytes. Arthritis Res Ther. 13(3):R93.

Bobinac D, Spanjol J, Zoricic S, Maric I. 2003. Changes in articular cartilage and subchondral bone histomorphometry in osteoarthritic knee joints in humans. Bone. 32(3):284–290.

Cao J, Zhang Y, Wang T, Li B. 2018. Endoplasmic reticulum stress is involved in baicalin protection on chondrocytes from patients with osteoarthritis. Dose Response. 16(4):1559325818810636.

Chen C, Chen H. 2019. Clinical diagnosis value of miR-29b-3p in peripheral blood mononuclear cells and synovial fluid among osteoarthritis patients. Clin Lab. 65.

Chen L, Li Q, Wang J, Jin S, Zheng H, Lin J, He F, Zhang H, Ma S, Mei J, et al. 2017. MiR-29b-3p promotes chondrocyte apoptosis and facilitates the occurrence and development of osteoarthritis by targeting PGRN. J Cell Mol Med. 21(12):3347–3359.

Dolka I, Król M, Sapierzyński R. 2016. Evaluation of apoptosis-associated protein (Bcl-2, Bax, cleaved caspase-3 and p53) expression in canine mammary tumors: an immunohistochemical and prognostic study. Res Vet Sci. 105:124–133.

Findlay DM, Atkins GJ. 2014. Osteoblast–chondrocyte interactions in osteoarthritis. Curr Osteoporos Rep. 12(1):127–134.

Geurts J, Jurić D, Müller M, Schären S, Netzer C. 2018. Novel ex vivo human osteochondral explant model of knee and spine osteoarthritis enables assessment of inflammatory and drug treatment responses. Int J Mol Sci. 19(5):1314.

Goldring MB, Otero M, Plumb DA, Dragomir C, Favero M, El Hachem K, Hashimoto K, Roach HI, Olivotto E, Borzì RM, et al. 2011. Roles of inflammatory and anabolic cytokines in cartilage metabolism: signals and multiple effectors converge upon MMP-13 regulation in osteoarthritis. Eur Cell Mater. 21:202–220.

Guerne PA, Carson DA, Lotz M. 1990. IL-6 production by human articular chondrocytes. Modulation of its synthesis by cytokines, growth factors, and hormones in vitro. J Immunol. 144(2):499–505.

Haqqi TM, Anthony DD, Gupta S, Ahmad N, Lee MS, Kumar GK, Mukhtar H. 1999. Prevention of collagen-induced arthritis in mice by a polyphenolic fraction from green tea. Proc Natl Acad Sci U S A. 96(8): 4524–4529.

Héraud F, Héraud A, Harmand MF. 2000. Apoptosis in normal and osteoarthritic human articular cartilage. Ann Rheum Dis. 59(12):959–965.

Hou K, Li G, Zhao J, Xu B, Zhang Y, Yu J, Xu K. 2020. Bone mesenchymal stem cell-derived exosomal microRNA-29b-3p prevents hypoxic-ischemic injury in rat brain by activating the PTEN-mediated Akt signaling pathway. J Neuroinflammation. 17(1):46.

Jin L, Zhao J, Jing W, Yan S, Wang X, Xiao C, Ma B. 2014. Role of miR-146a in human chondrocyte apoptosis in response to mechanical pressure injury in vitro. Int J Mol Med. 34(2):451–463.

Kaya Z, Yayla M, Cinar I, Atila NE, Ozmen S, Bayraktutan Z, Bilici D. 2019. Epigallocatechin-3-gallate (EGCG) exert therapeutic effect on acute inflammatory otitis media in rats. Int J Pediatr Otorhinolaryngol. 124: 106–110.

Liao CR, Wang SN, Zhu SY, Wang YQ, Li ZZ, Liu ZY, Jiang WS, Chen JT, Wu Q. 2020. Advanced oxidation protein products increase TNF-α and IL-1β expression in chondrocytes via NADPH oxidase 4 and accelerate cartilage degeneration in osteoarthritis progression. Redox Biol. 28:101306.

Liu YJ, Wang DY, Yang YJ, Lei WF. 2017. Effects and mechanism of dexmedetomidine on neuronal cell injury induced by hypoxia–ischemia. BMC Anesthesiol. 17(1):117.

Livak KJ, Schmittgen TD. 2001. Analysis of relative gene expression data using real-time quantitative PCR and the 2(–delta delta C(T)) method. Methods. 25(4):402–408.

Loening AM, James IE, Levenston ME, Badger AM, Frank EH, Kurz B, Nuttall ME, Hung HH, Blake SM, Grodzinsky AJ, et al. 2000. Injurious mechanical compression of bovine articular cartilage induces chondrocyte apoptosis. Arch Biochem Biophys. 381(2):205–212.

López-Armada MJ, Caramés B, Lires-Deán M, Cillero-Pastor B, Ruiz-Romero C, Galdo F, Blanco FJ. 2006. Cytokines, tumor necrosis factor-alpha and interleukin-1beta, differentially regulate apoptosis in osteoarthritis cultured human chondrocytes. Osteoarthritis Cartilage. 14(7):660–669.

Manka SW, Bihan D, Farndale RW. 2019. Structural studies of the MMP-3 interaction with triple-helical collagen introduce new roles for the enzyme in tissue remodelling. Sci Rep. 9(1):18785.

McAlindon TE, Bannuru RR, Sullivan MC, Arden NK, Berenbaum F, Bierma-Zeinstra SM, Hawker GA, Henrotin Y, Hunter DJ, Kawaguchi H, et al. 2014. OARSI guidelines for the non-surgical management of knee osteoarthritis. Osteoarthritis Cartilage. 22(3):363–388.

Mekky RY, El-Ekiaby N, El Sobky SA, Elemam NM, Youness RA, El-Sayed M, Hamza MT, Esmat G, Abdelaziz AI. 2019. Epigallocatechin gallate (EGCG) and miR-548m reduce HCV entry through repression of CD81 receptor in HCV cell models. Arch Virol. 164(6):1587–1595.

Mengshol JA, Vincenti MP, Coon CI, Barchowsky A, Brinckerhoff CE. 2000. Interleukin-1 induction of collagenase 3 (matrix metalloproteinase 13) gene expression in chondrocytes requires p38, c-Jun N-terminal kinase, and nuclear factor kappaB: differential regulation of collagenase 1 and collagenase 3. Arthritis Rheum. 43(4):801–811.

Mirzamohammadi F, Papaioannou G, Kobayashi T. 2014. MicroRNAs in cartilage development, homeostasis, and disease. Curr Osteoporos Rep. 12(4): 410–419.

Murphy NJ, Eyles JP, Hunter DJ. 2016. Hip osteoarthritis: etiopathogenesis and implications for management. Adv Ther. 33(11):1921–1946.

Ondrésik M, Azevedo Maia FR, da Silva Morais A, Gertrudes AC, Dias Bacelar AH, Correia C, Gonçalves C, Radhouani H, Amandi Sousa R, Oliveira JM, et al. 2017. Management of knee osteoarthritis. Current status and future trends. Biotechnol Bioeng. 114(4):717–739.

Pasquinelli AE. 2012. MicroRNAs and their targets: recognition, regulation and an emerging reciprocal relationship. Nat Rev Genet. 13(4):271–282.

Rasheed Z, Anbazhagan AN, Akhtar N, Ramamurthy S, Voss FR, Haqqi TM. 2009. Green tea polyphenol epigallocatechin-3-gallate inhibits advanced glycation end product-induced expression of tumor necrosis factor-alpha and matrix metalloproteinase-13 in human chondrocytes. Arthritis Res Ther. 11(3):R71.

Rasheed Z, Rasheed N, Al-Shaya O. 2018. Epigallocatechin-3-O-gallate modulates global microRNA expression in interleukin-1β-stimulated human osteoarthritis chondrocytes: potential role of EGCG on negative co-regulation of microRNA-140-3p and ADAMTS5. Eur J Nutr. 57(3):917–928.

Rasheed Z, Rasheed N, Al-Shobaili HA. 2016. Epigallocatechin-3-O-gallate up-regulates microRNA-199a-3p expression by down-regulating the expression of cyclooxygenase-2 in stimulated human osteoarthritis chondrocytes. J Cell Mol Med. 20(12):2241–2248.

Saklatvala J. 1986. Tumour necrosis factor alpha stimulates resorption and inhibits synthesis of proteoglycan in cartilage. Nature. 322(6079):547–549.

Sethi S, Li Y, Sarkar FH. 2013. Regulating miRNA by natural agents as a new strategy for cancer treatment. Curr Drug Targets. 14(10):1167–1174.

Shi X, Ye H, Yao X, Gao Y. 2017. The involvement and possible mechanism of NR4A1 in chondrocyte apoptosis during osteoarthritis. Am J Transl Res. 9:746–754.

Singh R, Akhtar N, Haqqi TM. 2010. Green tea polyphenol epigallocatechin-3-gallate: inflammation and arthritis. [corrected]. Life Sci. 86(25–26): 907–918.

World Medical Association. 2013. World Medical Association Declaration of Helsinki: ethical principles for medical research involving human subjects. JAMA. 310:2191–2194.

Wu Z, Luan Z, Zhang X, Zou K, Ma S, Yang Z, Feng W, He M, Jiang L, Li J, et al. 2019. Chondro-protective effects of polydatin in osteoarthritis through its effect on restoring dysregulated autophagy via modulating MAPK, and PI3K/Akt signaling pathways. Sci Rep. 9(1):13906.

Xia T, Dong S, Tian J. 2020. miR-29b promotes the osteogenic differentiation of mesenchymal stem cells derived from human adipose tissue via the PTEN/AKT/β-catenin signaling pathway. Int J Mol Med. 46(2):709–717.

Xiao D, Bi R, Liu X, Mei J, Jiang N, Zhu S. 2019. Notch signaling regulates MMP-13 expression via Runx2 in chondrocytes. Sci Rep. 9(1):15596.

Yan S, Wang M, Zhao J, Zhang H, Zhou C, Jin L, Zhang Y, Qiu X, Ma B, Fan Q. 2016. MicroRNA-34a affects chondrocyte apoptosis and proliferation by targeting the SIRT1/p53 signaling pathway during the pathogenesis of osteoarthritis. Int J Mol Med. 38(1):201–209.

Yoshimura H, Yoshida H, Matsuda S, Ryoke T, Ohta K, Ohmori M, Yamamoto S, Kiyoshima T, Kobayashi M, Sano K. 2019. The therapeutic potential of epigallocatechin-3-gallate against human oral squamous cell carcinoma through inhibition of cell proliferation and induction of apoptosis: in vitro and in vivo murine xenograft study. Mol Med Rep. 20(2): 1139–1148.

Zamli Z, Adams MA, Tarlton JF, Sharif M. 2013. Increased chondrocyte apoptosis is associated with progression of osteoarthritis in spontaneous Guinea pig models of the disease. Int J Mol Sci. 14(9):17729–17743.

Zan L, Chen Q, Zhang L, Li X. 2019. Epigallocatechin gallate (EGCG) suppresses growth and tumorigenicity in breast cancer cells by downregulation of miR-25. Bioengineered. 10(1):374–382.

Zeng L, Wang W, Rong XF, Zhong Y, Jia P, Zhou GQ, Li RH. 2014. Chondroprotective effects and multi-target mechanisms of icariin in IL-1 beta-induced human SW 1353 chondrosarcoma cells and a rat osteoarthritis model. Int Immunopharmacol. 18(1):175–181.

Zheng Y, Xiao L, Yu C, Jin P, Qin D, Xu Y, Yin J, Liu Z, Du Q. 2019. Enhanced antiarthritic efficacy by nanoparticles of (–)-epigallocatechin gallate-glucosamine-casein. J Agric Food Chem. 67(23):6476–6486.

Zhi L, Zhao J, Zhao H, Qing Z, Liu H, Ma J. 2021. Downregulation of LncRNA OIP5-AS1 induced by IL-1β aggravates osteoarthritis via regulating miR-29b-3p/PGRN. Cartilage. 13(2 Suppl.):1345S–1355S.